International Journal on Robotics, Automation and Sciences

Conditional Noise Filter for MRI Images with Revised Theory on Second-order Histograms

Wai Ti Chan*

***Abstract* - Previous research by the author has the theory that histograms of second-order derivatives are capable of determining differences between pixels in MRI images for the purpose of noise reduction without having to refer to ground truth. However, the methodology of the previous research resulted in significant false negatives in determining which pixel is affected by noise. The theory has been revised in this article through the introduction of an additional Laplace curve, leading to comparisons between the histogram profile and two curves instead of just one. The revised theory is that differences between the curve and histogram profile and the differences between the second curve and the profile can determine which pixels are to be selected for filtering in order to improve image clarity while minimizing blurring. The revised theory is tested with a modified average filter versus a generic average filter, with PSNR and SSIM for scoring. The results show that for most of the sample MRI images, the theory of pixel selection is more reliable at higher levels of noise but not as reliable at preventing blurring at low levels of noise.**

Keywords*— *Histograms, MRI Images, Modified Average Filter, Laplace Curves, Second-Order Derivatives

I. Introduction

This article is preceded by three other related works, which focus on the utilization of histograms of second-order derivatives of pixel values in an image[1][2][3]. All three works utilize second-order derivatives of pixel values, obtained from applying a distinct Laplace operator to a pixel and its neighbours. These works also use the observation that the frequency histogram of the aforementioned second-order derivatives resembles a Laplace curve. The theory behind these works is that the differences between the curve and the histogram profile can determine which pixel is affected by noise or low contrast. This paper utilizes the same ideas.

However, the first and second related works used just one Laplace curve that is made using the standard deviation of the distribution of the second-order derivatives. Although there are consistencies in the results, such as variables that are observed to be proportional to the level of noise, control tests with ground truth images showed that there were considerable false negatives, i.e. the methodology that was used did not select some pixels that happen to be affected by noise. This article intends to revise the theory behind the first and second works.

II. Review of Previous Works & Revision of Theory

The third of the previous works established the basis for the revision [3]. Analysis of the data in that work revealed that the previous theory of differences between just one Laplace curve and the histogram profile is not sufficient to avoid false negatives and false positives. That work led to the use of a different Laplace curve that is made using the peak frequency of the histogram profile. In the preliminary work for the research in this article, the third of the previous work was reexamined with the use of ground truth images.

*Corresponding author. Email: wtchan@mmu.edu.my, ORCID: 0000-0002-2366-1851
Wai Ti Chan is with the Faculty of Engineering and Technology (FET), Multimedia University (MMU), Jalan Ayer Keroh Lama, Bukit Beruang, 75450 Melaka, Malaysia. (e-mail: wtchan@mmu.edu.my).

International Journal on Robotics, Automation and Sciences (2021) 3:26-33
https://doi.org/10.33093/ijoras.2021.3.5
Manuscript received: 2 July 2021 | Revised: 27 Aug 2021 | Accepted: 9 Sep 2021 | Published: 8 Nov 2021

Published by MMU PRESS. URL: http://journals.mmupress.com/ijoras

The results of this reexamination is in Section E of Methodology.

Hence, this article proposes the use of more than one curve. The first curve, which is generated with the standard deviation of the distribution of the derivatives, is retained. A second curve is generated with the peak frequency of the histogram profile. Thus, the theory in this article is the merger of the theories in the previous works. Differences between the histogram profile and the two curves are used as the factors for a noise filter that selects pixels for average filtering

III. METHODOLOGY

A. Samples of MRI Images

The testing of the method that is proposed in this article uses a set of MRI images that are 150 in total from sources that include Radiopaedia and The Cancer Imaging Archives (TCIA). This set has been used in previous works [1][2][3]. The set includes images with many different image subjects. The images of the subjects were taken in different conditions and some have text and labels, among other visual diversity. This diversity has been useful for model training [4] and were so for the previous works, in which certain images revealed anomalies in the process flow of the methods.

B. Second-order Derivatives & Their Histograms

The use of second-order derivatives of pixel values and the frequency histograms of these derivatives have been elaborated in previous works [1][2][3]. For the sake of brevity and to avoid repetition, they will not be mentioned here. However, the use of two curves instead of just one in the methodology of this article still relies on the theory that noise contributes to the differences between the histogram profile and the curves.

C. Laplace Curves on the Histogram

As in previous works, there is a Laplace curve that is made using the standard deviation of the distribution of second-order derivatives [1][2][3]. This curve has been instrumental to applications of the aforementioned theory and remains so in the method that is proposed in this article. For ease of reference, this curve is referred to as the "first curve".

A second Laplace curve is introduced in the revision of the theory. This Laplace curve is generated such that its peak coincides with the top of the frequency interval of the second-order derivative value of zero. This is the curve that is used as the core of the termination conditions that are described in the third of the previous works [3]. It is used in the proposed method too. For ease of reference, the curve is referred to as the "second curve".

D. Differences between Heights of First and Second Curves and Heights of Histogram Intervals

The first and second of the previous works utilize the differences between the histogram profile and the first Laplace curve. The following is a recitation of equations that have been described in these works [1][2].

$$x_{1,j} = h_{1,j} - f_j \quad (1)$$

Where j is a distinct second-order derivative value,
f_j is the frequency of j,
$h_{1,j}$ is the height of the first curve at the location of j, and
$x_{1,j}$ is the difference between the height and the frequency.

The third of the previous works utilizes the differences between the profile and the second Laplace curve. The equation that is used for the differences is similar.

$$x_{2,j} = h_{2,j} - f_j \quad (2)$$

where f and j have been described in Equation (1), $h_{2,j}$ is the height of the second curve at the location of j, and $x_{2,j}$ is the difference.

These differences as described in Equations (1) and (2) are part of the hypotheses for the method that is proposed in this article. The hypotheses are described in the next two sections.

A reminder here is that the calculations in Equations (1) and (2) are performed for every image, be it the ground truth or its versions that have Rician noise introduced into them.

E. First Hypothesis

The aforementioned preliminary work, which is the reexamination of the third of previous work, resulted in the first hypothesis of the proposed method. The first hypothesis considers the following conditions that a pixel has with regard to its second-order derivative value, the frequency of that distinct value and the heights of the points on the curves that correspond to the second-order derivative value. These conditions are similar to the conditions that are described in the third previous work [3].

Condition No. 1: The second-order derivative value of the pixel has a frequency that is below the corresponding frequencies of both Laplace curves.

Condition No. 2: The second-order derivative value of the pixel has a frequency that is above the corresponding frequencies of both Laplace curves

Figure 1(a) shows one of the MRI images that were used in the preliminary work. Incidentally, this is the image that was featured in the previous works. Its second-order histogram and Laplace curves happen to be convenient for illustrating methodologies in the previous works. It is just as useful here.

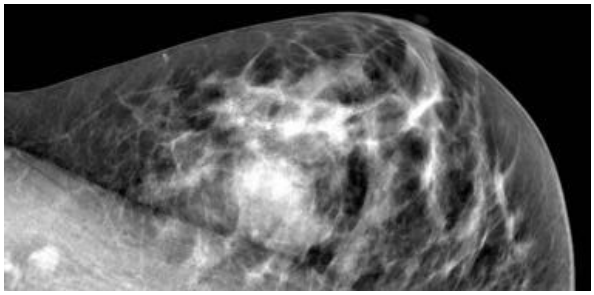

FIGURE 1 (a). MRI image of breast fibroadenoma

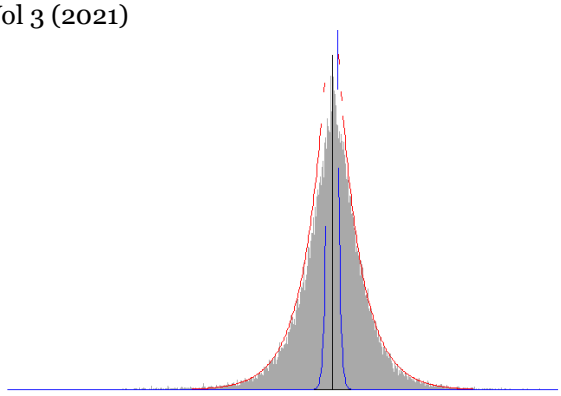

FIGURE 1 (b). Histogram of 2nd-order derivatives for Fig1(a)

Figure 1(b) shows the histogram of second-order derivative values for the image in Figure 1(a). The curve that is labeled σ_1 is the first curve, whereas the curve that is labeled σ_2 is the second curve; the first and second curves have been described earlier in section *C*. σ_1 is also the standard deviation of the distribution of the second-order derivatives. σ_2 is the standard deviation that is derived from the Laplace probability distribution function (PDF) for the second curve.

The number of pixels that meet the aforementioned conditions is determined. The results for the image in Figure 1(a) are shown in Table 1. Next, the percentages of pixels that meet the two conditions and are affected by noise are determined. This is done by referring to the ground truth image. Table 2 shows the results for the image in Figure 1(a).

The percentages in Table 2 are observed to be under those in Table 1, in terms of magnitude. This is expected because not all of the pixels that meet conditions no. 1 and 2 are affected by noise. However, since the percentages in both Tables are based on the total number of pixels in the image, the percentages in Table 2 are not significantly far from those in Table 1, especially at higher levels of noise. In other words, the pixels that meet conditions no. 1 and 2 do indicate the severity of noise. A reminder here is that conditions no. 1 and 2 do not make use of the ground truth image.

Furthermore, the summed percentages of pixels that meet conditions no. 1 and 2 and are affected by noise in Table 2 happen to approach 100% as noise levels become higher.

Thus, the first hypothesis of this article is that the number of pixels that meet conditions no. 1 and 2 can be used to estimate the amount of pixels to be selected for filtering. The caveat of which pixels to select is addressed by the second hypothesis.

F. Second Hypothesis

The second hypothesis of the proposed method considers how the level of noise affects pixels across the breadth of the histogram of second-order derivatives. The foreknowledge that is needed for this hypothesis is the effect of noise on the second-order

TABLE 1. Percentages of pixels in MRI image of Figure 1(a) that meet conditions no. 1 & 2 as noise level increases.

Standard deviation of distribution of Rician noise introduced into MRI image in Figure 1(a)	Percentages of pixels in MRI image of figure 1(a) that meet the conditions involving differences between histogram intervals and Laplace curves	
	Condition no. 1	***Condition no. 2***
2	42.22%	28.78%
4	38.91%	58.40%
6	35.04%	63.48%
8	31.48%	66.39%
10	29.93%	66.18%
12	30.89%	64.45%
16	33.33%	65.55%
20	32.71%	65.80%

TABLE 2. Percentages of pixels in MRI image of Figure 1(a) that meet conditions no. 1 & 2 and are affected by noise as noise level increases.

Standard deviation of distribution of Rician noise introduced into MRI image in Figure 1(a)	Percentages of pixels in MRI image of Figure 1(a) that meet the conditions involving differences between histogram intervals and Laplace curves and are affected by noise	
	Condition no. 1	***Condition no. 2***
2	32.59%	24.45%
4	34.48%	52.87%
6	32.17%	59.46%
8	29.21%	63.37%
10	28.12%	63.80%
12	29.33%	62.50%
16	31.88%	64.03%
20	31.55%	64.52%

derivatives of the pixels, which has been demonstrated in the first of the previous works [1].

To reiterate that previous work, at low levels of noise, the changes in the second-order derivative values are small, such that the effects are most significant in pixels that have similar intensity values, e.g. pixels with near-zero second-order derivatives. At higher levels of noise, the effects of noise are more severe such that pixels with second-order derivative values that are significantly greater in magnitude than zero, i.e. pixels further away from the vertical axis of the histogram, are affected by noise.

Therefore, the second hypothesis is that the selection of pixels should begin with pixels that have second-order derivative values of near-zero, before moving on to pixels with second-order derivatives of higher magnitudes.

G. Selection of Pixels

Pixels in the image are to be selected according to the stipulations as mentioned in the hypotheses. The extent of the pixels that are selected is determined by the ratio of pixels that meet conditions no. 1 and 2 to the total number of pixels that are on either side of the histogram. This ratio is calculated according to Equation (3).

$$R_{<0} = \frac{n_{1,j<0} + n_{2,j<0}}{\sum N_{j<0}} \quad (3)$$

Where $R_{<0}$ is the aforementioned ratio for the left side of the histogram, i.e. the side with distinct second-order derivative values that are negative,
$j<0$ represents a distinct second-order derivative value that is negative,
$\Sigma N_{j<0}$ is the total number of distinct second-order derivative values that are negative,
$n_{1,\,j<0}$ and $n_{2,\,j<0}$ are the numbers of distinct second-order derivative values that are negative, and which respectively meet conditions no. 1 and 2 as described in section *E*.

Equation (4), which is the converse of Equation (3), is for the distinct second-order derivative values that are positive, i.e. the right side of the histogram.

$$R_{>0} = \frac{n_{1,j>0} + n_{2,j>0}}{\sum N_{j>0}} \quad (4)$$

For emphasis, the ratios of $R_{<0}$ and $R_{>0}$ are not based on numbers of pixels. Rather, they are based on the number of distinct second-order derivative values.

$$N_{R,j<0} \approx (R_{<0})\left(n_{1,j<0} + n_{2,j<0}\right) \quad (5)$$

$$N_{R,j>0} \approx (R_{>0})\left(n_{1,j>0} + n_{2,j>0}\right) \quad (6)$$

Each ratio is then multiplied with the sum of n_1 and n_2 for its respective side of the histogram to give the number of distinct second-order derivative values that will be targets of the pixel selection process. This number is $N_{R,\,j>0}$ for the positive side of the histogram and $N_{R,\,j<0}$ for the negative side as described in Equations (5) and (6).

$$-N_{R,j>0} \leq j < 0 \quad (7)$$

$$0 < j \leq N_{R,j>0} \quad (8)$$

The numbers are then used to designate the distinct second-order derivative values that will be part of the pixel selection process. Equations (7) and (8) show the ranges of values that will be targeted. Any pixels with second-order derivative values that are within these ranges will be selected for average filtering.

This has been implemented as a response to the findings of the preliminary work as described in Tables 1 and 2, which is that not every pixel is affected by noise. A similar hypothesis has been posed in a previous work about noise reduction, in which the pixels with second-order derivative values that are closer to zero are processed before the others [2].

H. PSNR, SSIM & Control Tests

As in the previous works, PSNR and SSIM scores are used to measure the results of the tests. The scores are calculated by using the aforementioned 150 sample MRI images as ground truth images.

The control tests are performed using a generic average filter, which is typically applied on every pixel; this is otherwise known as the mean filter. Variants and modifications of the average filter have been used in the history of image processing because of the convenience of their implementation in programming and effectiveness on correcting pixels with significant noise [5]. Control tests for these filters use the generic average filter for comparing their results with those of the generic original, so the work that is described in this article does the same.

I. Goal of Testing

Ideally, the proposed conditions for selecting pixels for average filtering is to select pixels that are affected by noise while avoiding the pixels that are not. However, this is not possible without referring to the ground truth image [6]. Attempts like the preliminary work, as described in Table 2, could not produce a reliable method of identifying pixels that are affected with noise without the aforementioned referral.

Thus, the goal of the test would involve measuring the PSNR and SSIM scores of the results of both sets of tests, and comparing them with each other. The outcome is considered to be in the favor of the proposed methodology if the PSNR and SSIM scores for the tests with the methodology are consistently higher than those for the control tests.

IV. Results & Discussion

A. Example of Filtering with the Proposed Methodology

The MRI image in figure 1(a) and its noisy versions are used as an example to demonstrate the results of the filtering. Tables 3 and 4 show the results for the tests on the image. The results for the tests with the proposed method are represented by the second and third columns from the left in Tables 3 and 4. Results of the tests with the control tests are represented by the fourth and fifth columns.

Table 3 shows that the proposed method does not always produce higher PSNR and SSIM results for every level of noise for this MRI image. Similar results would be had for other specific MRI images too, thus suggesting that the image subject is a factor. Incidentally, this finding has occurred in two of the previous works as well [2][3].

However, when the results across the 150 sample

images and their noisy variants are considered, there is a trend of the proposed method producing generally higher PSNR and SSIM scores than the control tests.

TABLE 3. PSNR & SSIM scores for the MRI image in Figure 1(a) across Rician noise levels of standard deviation of 2 to 10.

Scores	Standard deviation of noise distribution in noisy MRI image			
	2	***4***	***6***	***8***
PSNR before filtering	42.35	36.48	33.01	30.43
SSIM before filtering	0.999	0.998	0.996	0.993
PSNR after filtering with proposed method	38.18	33.93	33.55	32.61
SSIM after filtering with proposed method	0.999	0.997	0.997	0.996
PSNR after filtering with control test	35.45	34.62	33.51	32.23
SSIM after filtering with control test	0.998	0.997	0.997	0.995

B. Results of Tests on Sample MRI Images

Table 5 shows the results across the 150 sample MRI images. In the case of these results, the exact PSNR and SSIM scores for each image and its noisy versions have been omitted for the sake of brevity. Instead, the results are tabulated according to the method shown in Tables 5 and 6.

The results in both tables have been arranged according to levels of Rician noise so as to examine the effectiveness of the proposed method as noise increases in severity.

The data in Table 5 is obtained from the ratio of the PSNR score achieved by the proposed method to the score achieved by the control test. Ratios are used instead of numerical differences because of the wide variation in the scores due to the use of images with varying image subjects. To present the results across the sample images, the average of the ratios and their standard deviation are calculated for each level of noise [7]. The table also includes a column on the number of images where the ratio is less than 1, i.e. where the control test performed better.

The data in Table 6 is obtained from the difference between the SSIM score achieved by the proposed method and the score achieved by the control test. Since the range for the SSIM score is limited between zero and unity, these differences are sufficient for the presentation of the data. As in Table 5, averages and standard deviations of the differences are calculated for each level of noise. There is also a column on the number of images where the difference is negative, i.e. where the proposed method performed worse.

Both Tables 5 and 6 show that the proposed method of selecting pixels with the use of histograms of second-order derivatives generally has better performance than the control test across all levels of noise. The performance also improves with increasing

TABLE 4. PSNR & SSIM scores for the MRI image in Figure 1(a) across Rician noise levels of standard deviation of 12 to 20.

Scores	Standard deviation of noise distribution in noisy MRI image			
	10	***12***	***16***	***20***
PSNR before filtering	28.40	26.78	24.09	22.27
SSIM before filtering	0.989	0.984	0.971	0.949
PSNR after filtering with proposed method	31.35	30.71	28.45	24.47
SSIM after filtering with proposed method	0.994	0.994	0.989	0.967
PSNR after filtering with control test	30.99	29.79	27.57	23.84
SSIM after filtering with control test	0.994	0.992	0.987	0.961

TABLE 5. PSNR scoring for tests across the 150 sample MRI images.

Standard deviation of noise distribution	Average of ratios of PSNR scores by the proposed test over the PSNR scores by the control tests	Standard deviation of ratios of PSNR scores by the proposed test over the PSNR scores by the control tests	Number of images where the proposed test has lesser performance than the control test
2	1.0886	0.1425	40
4	1.0676	0.1145	33
6	1.0582	0.0923	19
8	1.0528	0.0757	17
10	1.0518	0.0640	17
12	1.0545	0.0566	14
16	1.0653	0.0438	9
20	1.0730	0.0417	7

levels of noise, as indicated by the increasing averages in both Tables. Furthermore, the decreasing magnitudes of the standard deviations in both Tables suggest that the reliability of the proposed method improves as noise levels increase.

As a reminder, blurring can occur for images with low levels of noise if a noise filter selects more pixels for processing than it should. The control test uses a typical average filter, so it is selecting every pixel there is in an image. The proposed method does not select all of them, as mentioned earlier in the Methodology section; ideally, this should result in less blurring.

However, the data that is represented by the fourth column in both Tables has been included to determine

any setback or caveat in the proposed method. From this data in the results, the proposed method evidently could not prevent blurring at low levels of noise and more importantly, it has not selected many of the pixels that are affected by noise; the control test certainly has included these pixels for processing, so the control test performed better for these images.

On the other hand, the same columns also show that the number of images where the proposed method has lesser performance decreases as the noise level increases, thus further reinforcing the aforementioned impression that the proposed method has improved performance and reliability as noise levels increase.

TABLE 6. PSNR scoring for tests across the 150 sample MRI images.

Standard deviation of noise distribution	Average of differences between SSIM scores by the proposed test and the SSIM scores by the control tests	Standard deviation of differences between SSIM scores by the proposed test and the SSIM scores by the control tests	Number of images where the proposed test has lesser performance than the control test
2	0.0049	0.0194	39
4	0.0047	0.0191	31
6	0.0049	0.0187	20
8	0.0050	0.0183	18
10	0.0052	0.0177	18
12	0.0058	0.0174	14
16	0.0083	0.0154	8
20	0.0114	0.0142	7

C. Checks on False Negatives and False Positives

The proposed method is not subjecting every pixel to average filtering, i.e. it is selecting specific pixels as described in section G of the Methodology. Thus, the pixels that are selected have to be checked against the corresponding pixels in the ground truth image for any presence of noise that has been introduced in the noisy versions of the ground truth images [8].

Specifically, the values of the pixels that have been selected are compared with those of their counterparts in the ground truth image. If they are equal, this is a false positive, i.e. the proposed method has selected a pixel that does not have noise introduced to it. The values of the pixels that have not been selected are also compared with those of their counterparts. If they are not equal, this is a false negative, i.e. the proposed method did not select a pixel that has noise introduced to it.

To present the data of these checks across the sample images, the amounts of false negatives and false positives are presented as a percentage of the number of false negatives to the total number of pixels that are not selected, whereas the amount of false positives are presented as a percentage of the number of false positives to the total number of pixels that are targeted. For juxtaposition, the amounts of false negatives and positives are also presented as percentages of the total number of pixels in an image. The results are shown in Tables 7 and 8.

According to Table 7, the proposed method exhibits less false positives on average as noise levels increase. However, the standard deviation does not share the same trend.

TABLE 7. False positives and false negatives, according to noise level and percentage of pixels selected and not selected.

Standard deviation of noise distribution	Average percentage (%)[a] of pixels with false positives and standard deviation	Average percentage (%)[b] of pixels with false negatives and standard deviation
2	24.05 ± 7.39	78.03 ± 4.11
4	14.87 ± 7.23	88.08 ± 4.26
6	11.63 ± 7.18	91.20 ± 4.59
8	9.99 ± 7.14	92.62 ± 4.71
10	8.99 ± 7.11	93.17 ± 5.11
12	8.32 ± 7.10	93.55 ± 5.24
16	7.50 ± 7.09	93.78 ± 5.75
20	7.06 ± 7.15	94.19 ± 6.03

a. The percentage is calculated according to the fraction of the pixels that have false positives over the number of pixels that have been selected for filtering.
b. The percentage is calculated according to the fraction of the pixels that have false negatives over the number of pixels that have not been selected for filtering.

This suggests that the decreasing average is not a sign of improving performance at avoiding false positives. Instead, the increasing proportion of pixels that are affected by noise as the noise level increases would mean that most of the pixels that the proposed method would select are already affected by noise, thus reducing the possibility of a false positive.

This impression is further reinforced with the finding that the average percentage of false negatives increases as noise level increases. As the noise level increases, there are fewer pixels that are not affected by noise, so the likelihood of a pixel that is not selected having noise increases.

Table 8 is included here to allay the impression that the proposed method fares poorly at avoiding false outcomes. While Table 7 presents the percentages as percentages of the numbers of pixels that are or are not selected, Table 8 presents them as percentages of the total number of pixels in the image instead. From Table 8, the proposed method appears to have a trend of improvement as the noise level increases, if its performance is to be measured against the total number of pixels in the image instead of the numbers of pixels that have or have not been selected.

However, that the standard deviations for the percentages in Table 8 have opposing trends for false positives and false negatives would suggest that this seeming improvement is mainly due to there being more pixels that are affected by noise and fewer pixels that are not, as mentioned earlier. In other words, the proposed method has fewer occurrences for false negatives and negatives as noise level increases.

TABLE 8. False positives and false negatives, according to noise level and percentage of total number of pixels in an image.

Standard deviation of noise distribution	Average percentage (%)[c] of pixels with false positives and standard deviation	Average percentage (%)[d] of pixels with false negatives and standard deviation
2	21.32 ± 5.56	7.92 ± 7.10
4	13.53 ± 6.08	6.90 ± 6.99
6	10.78 ± 6.33	5.62 ± 6.51
8	9.40 ± 6.51	4.72 ± 6.40
10	8.56 ± 6.61	3.81 ± 5.51
12	8.00 ± 6.69	3.05 ± 4.58
16	7.30 ± 6.76	1.95 ± 2.67
20	6.89 ± 6.84	1.66 ± 2.55

c. The percentage is calculated according to the fraction of the pixels that have false positives over the total number of pixels in an image.
d. The percentage is calculated according to the fraction of the pixels that have false negatives over the total number of pixels in an image.

V. CONCLUSION

The proposed method of pixel selection through the use of statistical data from a histogram of second-order derivatives has significant performance and reliability at higher levels of noise when this is measured via PSNR and SSIM. The results also show that the revised theory of having two Laplace curves to compare the histogram against is more reliable than the previous theory of using only one curve that is based on the standard deviation of the distribution of the second-order derivative values of the pixels in the image.

However, when the performance of the method is measured according to whether the pixel that is selected for filtering is affected by noise or not, the finding is that the proposed method performs better at filtering pixels with noise at higher levels of noise by virtue of there being more pixels with noise that it would select. Yet, the performance of the method when measured in comparisons of PSNR and SSIM would suggest that selecting pixels through analysis of the second-order histogram is a viable choice.

In other words, there is space for improvement, namely how the selection algorithm could be modified further in order to provide an estimate of the noise that may be possibly affecting a pixel. The introduction of the second Laplace curve as another variable in the analysis supports the notion that more distinctly different types of data from the histogram is needed in order to improve the reliability of any theories that utilize a histogram of second-order derivative values of pixels for the processing of an image.

ACKNOWLEDGMENT

We thank the anonymous reviewers for the careful review of our manuscript.

FUNDING STATEMENT

There is no funding agencies supporting the research work,

AUTHOR CONTRIBUTIONS

Wai Ti Chan: Conceptualization, Data Curation, Methodology, Validation, Writing – Original Draft Preparation, Project Administration, Supervision, Writing – Review & Editing.

CONFLICT OF INTERESTS

No conflict of interests were disclosed.

ETHICS STATEMENTS

Our publication ethics follow The Committee of Publication Ethics (COPE) guideline. https://publicationethics.org/

REFERENCES

[1] W. T. Chan, K. S. Sim and F. S. Abas, “Contrast measurement with histograms of second-order derivatives of pixels for magnetic resonance images,” *Engineering Letters*, vol. 27, no. 2, pp. 390–395, 2019.
URL: https://www.engineeringletters.com/issues_v27/issue_2/EL_27_2_16.pdf (Accessed 20 Aug, 2021)

[2] W. T. Chan, K. S. Sim and F. S. Abas, “Pixel filtering and reallocation with histograms of second-order derivatives of pixel values for electron microscope images,” *International Journal of Innovative Computing, Information and Control*, vol. 14, no. 3, pp. 915–928, 2018.
DOI: https://doi.org/10.24507/ijicic.14.03.915

[3] W. T. Chan and K. S. Sim, “Termination factor for iterative noise reduction in MRI images using histograms of second-order derivatives,” *International Journal of Computer Science*, vol. 48, no. 1, pp. 174–180, 2021.
DOI: https://doi.org/10.1007/s00200-020-00512-w

[4] Y. Gao, Y. Y. Wang and J. H. Yu, “Optimized resolution-oriented many-to-one intensity standardization method for magnetic resonance images,” *Applied Sciences*, vol. 9, no. 24, p. 5531, 2019.
DOI: https://doi.org/10.3390/app9245531

[5] M. Kromrey, D. Tamada, H. Johno, S. Funayama, N. Nagata, S. Ichikawa, J. Kühn, H. Onishi and U. Motosugi, “Reduction of respiratory motion artifacts in gadoxetate-enhanced MR with a deep learning–based filter using convolutional neural

network," *European Radiology*, vol. 30, no. 11, pp. 5923-5932, 2020.
DOI: https://doi.org/10.1007/s00330-020-07006-1

[6] W. Burger and M. J. Burge, "Digital Image Processing," Texts in Computer Science, 2016.
DOI: https://doi.org/10.1007/978-1-4471-6684-9

[7] S. Imanaka and Y. Shibasaki, "A study of the incidence of hip fractures in post-menopausal patients undergoing hemodialysis using quantitative ultrasound, digital image processing and the fracture risk assessment tool," *Nippon Ronen Igakkai Zasshi. Japanese Journal of Geriatrics*, vol. 57, no. 1, pp. 81-88, 2020.
DOI: https://doi.org/10.3143/geriatrics.57.81

[8] M. Rottman, K. Maag, R. Chan, F. Hügger, P. Schlicht and H. Gottschalk, "Detection of false positive and false negative samples in semantic segmentation," 2019.
DOI: https://doi.org/10.48550/arXiv.1912.03673